PCCP

Accepted Manuscript

ROYAL SOCIETY OF CHEMISTRY

www.rsc.org/pccp

Physical Chemistry Chemical Physics

ARTICLE

Ion Transport in Polycarbonate Based Solid Polymer Electrolytes: Experimental and Computational Investigations

Received 00th January 20xx,
Accepted 00th January 20xx

DOI: 10.1039/x0xx00000x

www.rsc.org/

Bing Sun,[a] Jonas Mindemark,[a] Evgeny Morozov,[b] Luciano T. Costa,[c] Martin Bergman,[d] Patrik Johansson,[d] Yuan Fang,[b] István Furó,[b] Daniel Brandell[a,*]

Among the alternative host materials for solid polymer electrolytes (SPEs), polycarbonates have recently shown promising functionality in all-solid-state lithium batteries from ambient to elevated temperatures. While the computational and experimental investigations of ion conduction in conventional polyethers have been extensive, the ion transport in polycarbonates has been much less studied. The present work investigates the ionic transport behavior in SPEs based on poly(trimethylene carbonate) (PTMC) and its co-polymer with ε-caprolactone (CL) via both experimental and computational approaches. FTIR spectra indicated a preferential local coordination between Li^+ and ester carbonyl oxygen atoms in the P($TMC_{20}CL_{80}$) co-polymer SPE. Diffusion NMR revealed that the co-polymer SPE also displays higher ion mobilities than PTMC. For both systems, locally oriented polymer domains, a few hundred nanometers in size and with limited connections between them, were inferred from the NMR spin relaxation and diffusion data. Potentiostatic polarization experiments revealed notably higher cationic transference numbers in the polycarbonate based SPEs as compared to conventional polyether based SPEs. In addition, MD simulations provided atomic-scale insight to the structure–dynamics properties, including confirmation of a preferential Li^+–carbonyl oxygen atom coordination, with a preference in coordination to the ester based monomers. A coupling of the Li-ion dynamics to the polymer chain dynamics was indicated by both simulations and experiments.

Introduction

The growing demand for cost-effective electric portable power sources which utilize solvent-free solid electrolytes to improve safety has drawn extensive interest in the field of batteries.[1,2] By excluding the flammable and volatile organic solvents used in conventional electrolytes, solid polymer electrolytes (SPEs) possess better chemical stability and have commonly been considered for safer Li batteries, even though they exhibit lower ionic conductivities.[3–5] Considering the many requirements for battery electrolytes in terms of practical use – including suitable ionic conductivity over a wide temperature range and long-term cycleability, *etc*. – compromises between mechanical properties, fast ionic transport and safety aspects are necessary.[3,5–7]

Conventional polymer host materials for SPEs are derived from polyethers, *e.g*., poly(ethylene oxide) (PEO) and poly(propylene oxide) (PPO). These polymer structures have dominated the field for decades due to their favorable properties for salt solvation and ion conduction.[8] However, the ionic conductivity of their SPEs are low at ambient temperatures: 10^{-5}–10^{-8} S cm^{-1},[9] caused by semi-crystallinity and strong ion complexation.[9,10] Moreover, as indicated from both experimental and computational studies, the anionic dynamics generally supersedes the cationic dynamics, resulting in lithium transference numbers t_+<0.5, *e.g., ca.* 0.2–0.3 for PEO_xLiTFSI).[11,12] The reason is that the anion mobility is less restricted by the polymer segmental motions, as lithium cations are dominantly solvating with ether oxygen atoms along polymer chains, usually with a total coordination number (CN) of 5–6 as found from *ab initio*/DFT computations,[13] neutron diffraction experiments,[14] and molecular dynamics (MD) simulations.[15] In total, the first solvation shell of Li^+ in PEO_xLITFSI is composed by ether oxygen atoms, CN=3.85 and sulfonyl oxygen atoms from TFSI, CN=0.5.[15] A similar CN=3.8 was also obtained from MD simulations of Li^+–$O_{C=O}$ coordination in LiTFSI–ethylene carbonate (EC) electrolytes.[16]

One strategy to achieve fast ion transport in SPEs as previously investigated was to suppress the poorly conducting crystalline domains in low–T_g polymers such as polyethers. Alternative routes explored are for example to decouple the ionic motion from the polymer relaxation, both in crystalline and ordered polymer electrolytes[17–21] and in polymer-in-salt systems.[22,23] Among the various non-polyether materials suggested, polycarbonates – the

[a] Department of Chemistry – Ångström Laboratory, Uppsala University, Box 538, SE-75121, Uppsala, Sweden
[b] Division of Applied Physical Chemistry, Department of Chemistry, KTH Royal Institute of Technology, Teknikringen 36, SE-10044, Stockholm, Sweden
[c] Instituto de Química – Departamento de Físico-Química, Universidade Federal Fluminense, Outeiro de São João Batista s/n CEP 24020-150 Niterói – RJ, Brazil.
[d] Department of Physics, Chalmers University of Technology, SE-41296, Gothenburg, Sweden

Electronic Supplementary Information (ESI) available. See DOI: 10.1039/x0xx00000x

solid analogues to the liquid carbonate solvents, like EC, predominantly used in commercial Li-ion batteries – have shown favorable solvation of lithium salts.[24] As demonstrated in a

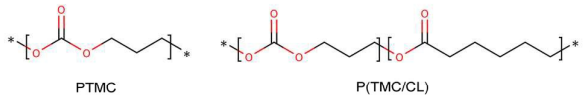

Fig.1 Chemical structures of PTMC and P(TMC/CL) co-polymers.

comparative study between poly(ethylene carbonate) (PEC) and PEO, both doped with lithium bis(fluorosulfonyl imide) (LiFSI), a significantly higher cationic transference number was observed for the LiFSI–PEC system, but its origin is not yet well understood.[24]

High-molecular-weight poly(trimethylene carbonate) (PTMC) (**Fig. 1**) and synthetic modifications thereof have successfully been used as matrices to create SPEs for all-solid-state Li polymer batteries operating from room-temperature to elevated temperatures (22–60 °C).[25–27] As PTMC is a more rigid polymer than PEO, $PTMC_x$LiTFSI has a T_g of *ca.* −16 °C and hence displays lower ionic conductivity than PEO–LiTFSI at close to ambient temperatures.[25] By varying the polymer architecture via co-polymerization, SPEs with ionic conductivities of up to 10^{-5} S cm^{-1} at ambient temperature could be realized, based on random co-polymers of TMC and ε-caprolactone (CL) units (P(TMC/CL)) (**Fig. 1**).[27,28] Compared to $PTMC_x$LiTFSI complexes which commonly display ionic conductivities of *ca*. 10^{-10} S cm^{-1} at ambient temperature, co-polymerization shows a significant enhancement in overall conductivity, yet its correlation with polymer dynamics and local coordination remains elusive. A clearer picture of the molecular level structure–dynamics properties would be beneficial to guide further molecular design towards high-performance battery electrolytes.

This paper presents studies aimed at understanding the ion transport mechanism in polycarbonate-based SPEs. Both experiments and computations were made on two polycarbonate systems: PTMC–LiTFSI, a "standard" polycarbonate system, and the co-polymer $P(TMC_{20}CL_{80})$–LiTFSI (*i.e.*, a TMC/CL monomer molar ratio of 20:80) which features enhanced conductivity at r.t. and beyond.[27] Insights on ion-association in both systems were gained from FTIR analysis and NMR relaxation, while potentiostatic polarization (PP) and diffusion NMR experiment were applied as complementary methods to characterize ionic diffusion coefficients and transference numbers. In order to get insights into the relationship between the local coordination environment and ion transport, MD simulations were performed and the results correlated with experimental data.

Experimental

Sample preparation

LiTFSI (Purolyte, from Ferro Corp.) was dried in a vacuum oven at 120 °C for 24 h prior to use. Anhydrous acetonitrile (Acros Organics) was used as received. The synthesis of high-molecular-weight PTMC and $P(TMC_{20}CL_{80})$ is described in detail elsewhere.[25,27,28] SPEs with optimized conductivities for each of the two systems; $PTMC_8$LiTFSI (*i.e.*, [TMC]:[Li^+]=8:1) and $P(TMC_{20}CL_{80})_{4.6}$LiTFSI ([$TMC_{20}CL_{80}$]:[Li^+]=4.6:1),[25,27] were studied. In addition, self-standing SPEs with different salt concentrations – $PTMC_8$LiTFSI and $P(TMC_{20}CL_{80})_y$LiTFSI (y = 4.6, 6.6) – were prepared. All SPEs were made by solution-casting and all sample preparation was performed in an argon-filled glove box.

Instruments and methods

Transference number measurements. Potentiostatic polarization measurements using procedures reported by Hiller *et al.*[29] were carried out using symmetric Li/SPE/Li cells with an electrode area of 1.13 cm^2 at 333 K. The transference numbers of $PTMC_8$LiTFSI and $P(TMC_{20}CL_{80})_{4.6}$LiTFSI were calculated using the equation by Evans *et al.*[30] All cells were thermally equilibrated for 15–20 h in an oven while the resistance was tracked until a stable cell resistance was observed. Temperature fluctuations were maintained within 0.25 K. Impedance and polarization measurements were analyzed by a VMP2 (Biologic) device. An ac bias of 10 mV within a frequency range of 1 Hz to 1 MHz was applied for electrochemical impedance spectroscopy (EIS) and a dc bias of 10 mV was used for polarization. The obtained data from the EIS were fitted by ZView (version 2.8d, Scribner Associates).

NMR diffusion and relaxation measurements. All NMR measurements were performed by using a Bruker AVANCE 500 MHz spectrometer equipped with a water-cooled gradient probe Diff 30 and a set of 10 mm radiofrequency coils tuned to ^{1}H (500 MHz), ^{19}F (470.4 MHz) and ^{7}Li (194.3 MHz) nuclei. The longitudinal (T_1) and transverse (T_2) relaxation measurements were carried out using the inversion recovery and Hahn spin-echo pulse sequences, respectively. The relaxation decays were well approximated by single-exponential functions; exception in the form of a significant (with decay component amplitudes in the same order of magnitude) multi-exponentiality is the ^{7}Li transverse relaxation. Diffusion coefficients were measured using the standard pulsed-field-gradient stimulated echo sequence with longitudinal eddy current delay.[31] Diffusion parameters were as follows: gradient pulse length, δ=1 ms; diffusion time, Δ=400 ms; maximum gradient strength g_{max}=15 T/m. Proton (^{1}H), fluorine (^{19}F) and lithium (^{7}Li) NMR relaxation were measured on $PTMC_8$LiTFSI and $P(TMC_{20}CL_{80})_{4.6}$LiTFSI in a temperature range of 295 K to 333 K. The cation and anion diffusion coefficients in the $P(TMC_{20}CL_{80})_{4.6}$LiTFSI were measured within a more narrow range of 323 K to 334 K. The limitation towards lower temperatures was caused by the shortening of T_2 there, ultimately leading to loss of signal in the stimulated-echo experiment. Yet, the data were sufficiently accurate to obtain accurate activation energies despite the limited range. In $PTMC_8$LiTFSI, the ^{7}Li signal was not suitable at all for diffusion measurements below *ca.* 360 K. For this reason, we purpose-built a high-temperature ^{7}Li radiofrequency insert for our water-cooled diffusion probe that permitted experiments up to 423 K. Hence, in $PTMC_8$LiTFSI the diffusion coefficient of the lithium ions

was obtained in the 363–423 K range. The thermal equilibration time at each sampling point was 30 min.

FTIR spectroscopy. The vibrational spectroscopy was performed at ambient temperature using a Bruker ALPHA FT-IR spectrometer and an ATR set-up (diamond crystal) inside an argon-filled glovebox. Each sample was measured as a self-standing membrane with a resolution of 2 cm^{-1} and 3500–7000 scans. The peaks were deconvoluted and fitted using the 'Voigt Amp' function and a linear baseline correction in PeakFit (version 4.04) by a stepwise release of fitting constraints starting from identical band shapes and widths.

Modeling. MD simulations were performed using a united-atom model for the CH_2 groups of PTMC and the co-polymer. The intra- and intermolecular parameters used are based on the ether and ester functional groups derived from OPLS force field.[32] The anion model was based on the non-scaled charge (NSC) force field used for modeling ionic liquids based on the bis(trifluoromethanesulfonyl)imide anion, TFSI.[33] The Li ion model was derived from the OPLS database in the GROMACS package.[34] The simulation boxes that contained 40 Li–TFSI ion pairs and 32 oligomer chains of PTMC or the co-polymer were built using the Packmol program.[35] Energy-minimization was achieved by the steepest-descent method followed by NVT ensemble simulations to decrease repulsive contacts. All production runs were at least 50 ns long using a time-step of 0.002 ps and a leap-frog algorithm. The simulations were performed under NPT conditions at 1 bar (with T_{bath} controlled using V-rescale; coupling time=0.1 ps, P_{bath} controlled using the Parrinello-Rahman method; coupling time=5 ps). A particle-mesh Ewald summation routine was used for long-range forces (r_{cut} = 14 Å), and data was collected for statistical analysis at every 200th time-step. Both PTMC and the co-polymer SPEs were modelled at temperatures 303 K, 348 K and 423 K.

Results and Discussion

First, the respective ion motions are discussed in correlation with the polymer motions by NMR, whereafter the Li ion coordination environment is examined by FTIR and the contribution of CL units is particularly investigated. Furthermore, complementary results of diffusion properties and transport number from both experiments and MD simulations are explored to uncover the ion transport mechanisms in the SPEs.

NMR relaxation studies

The longitudinal and transverse relaxation data are collected in **Figs. 2 and 3**, respectively. The ^{7}Li data arise from the lithium cation, the ^{19}F data from the TFSI anion, while the ^{1}H data is due to the polymer chains.[36] The longitudinal relaxation is related to molecular motions whose correlation time is comparable to the inverse of the relevant Larmor frequency. The relaxation mechanisms for the three explored nuclei are different from each other. For ^{7}Li, a spin I=3/2 nucleus, the relaxation is dominantly quadrupolar and, as customary for ions,[37,38] is dominated by the ps–ns dynamics of the coordination shell. For ^{1}H, the relaxation is caused by fluctuating dipole-dipole interactions, dominantly intramolecular within the polymer and connected to fast (<ns) segmental motions. Finally, the ^{19}F longitudinal relaxation is dominated by the spin-rotation mechanism, which renders the relaxation data dependent on the correlation time of the intramolecular rotation of the CF_3 group.[39] This is also the reason why the temperature dependence of the ^{19}F data is opposite to that of the ^{7}Li and ^{1}H data. Therefore, the ^{19}F longitudinal relaxation data do not report on dynamics relevant for ion transport and will not be discussed further.

One major possibility with the relaxation experiments is to study the influence of the polymer host on the ion dynamics. The temperature variation of T_1 for either ^{1}H or ^{7}Li displays no relaxation minimum, for ^{7}Li in $PTMC_8LiTFSI$ not even up to 423 K. Within the conventional framework,[40] this points to re-orientational

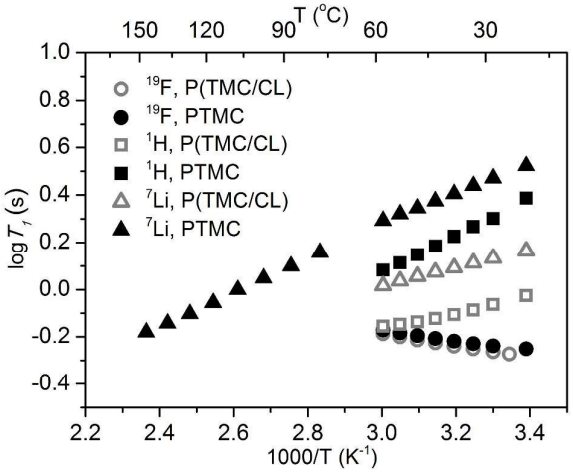

Figure 2. Temperature dependence of the longitudinal relaxation time (T_1) in both $PTMC_8LiTFSI$ (solid symbols) and $P(TMC_{20}CL_{80})_{4.6}LiTFSI$ (half-filled symbols). Different symbols represent ^{1}H (squares), ^{7}Li (triangles) and ^{19}F (circles) relaxation, respectively.

correlation times τ_c fulfilling the condition $\omega\tau_c > 1$, where ω is the Larmor frequency of the respective nucleus. Compared to semicrystalline PEO–LiX and amorphous PPO–LiX (X = ClO_4, TFSI),[11,41] this indicates slower re-orientational motions in the present system. While the value of τ_c cannot be obtained directly, apparent activation energies can be evaluated from the temperature dependence of T_1 (**Table S1**). Clearly, changing the polymer host strongly affects the local motions of ^{7}Li and the close values of the activation energies for ^{1}H and ^{7}Li relaxation in a given polymer indicate that the local motions of the lithium ion and the polymer host are closely correlated. Lower activation energies for the $P(TMC_{20}CL_{80})_{4.6}LiTFSI$ system indicate higher flexibility than in the $PTMC_8LiTFSI$ system. The activation energy of the polymer and lithium cation motion seems to decrease upon decreasing O:Li ratio where O indicates coordinating oxygen atoms,[39] which is in the same direction as the effect observed here, though probably cannot explain the difference between the activation energies observed in $P(TMC_{20}CL_{80})_{4.6}LiTFSI$ and $PTMC_8LiTFSI$. Furthermore, the exact

value of τ_c time also depends on the so-called pre-exponential factor (also expressed by its inverse, the attempt frequency).[42] In the present case, this must be assumed to be a complex function of the vibrations of the various coordinating groups.

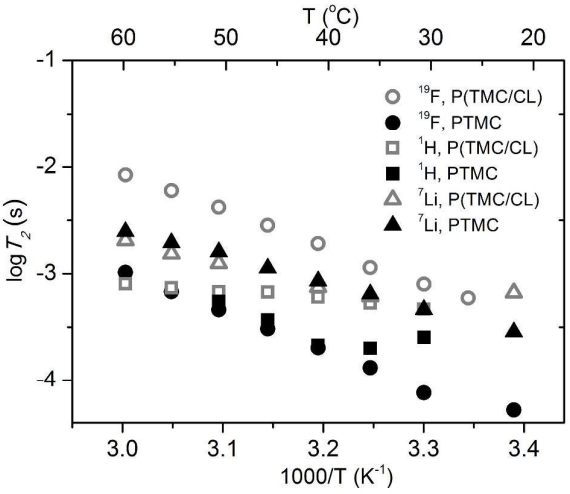

Fig. 3 Temperature dependence of the transverse relaxation time (T_2) of ^{19}F (circles), ^{7}Li (triangles) and ^{1}H (squares) for both $PTMC_8LiTFSI$ (solid symbols) and $P(TMC_{20}CL_{80})_{4.6}LiTFSI$ (empty symbols).

Fig. 3 summarizes the apparent transverse relaxation data (see also **Fig. S1** in Supporting Information). The transverse relaxation times for ^{1}H and ^{19}F are much, by two–three orders of magnitude, shorter than their longitudinal relaxation times, indicative of some slow motional modes modulating the relevant spin couplings, dominantly dipole–dipole for ^{1}H and ^{19}F. These slow motional modes need not (for ^{19}F, cannot) be connected to the fast motions causing the behavior of the longitudinal relaxation times. For both nuclei, T_2 generally (with some deviations at the lowest temperatures) increases upon increasing temperature which reflects that the involved molecular motions get faster. The ^{1}H T_2 values are also shorter for $PTMC_8LiTFSI$ than for $P(TMC_{20}CL_{80})_{4.6}LiTFSI$ which indicates faster motions in the latter and thus a more flexible system. This has also been reported in earlier studies on polyether-based SPEs, where the rapid conformal fluctuations of the crosslinks from cation–polymer segments were proposed to alter the dynamics of the polymer network.[43] There is a remarkably large difference between the T_2 values recorded in $PTMC_8LiTFSI$ on the one hand and $P(TMC_{20}CL_{80})_{4.6}LiTFSI$ on the other hand. This is indicative of faster anion dynamics in the latter system, which may be connected to the lack of ion pairing there as also inferred from the FTIR data (see **Fig. 6** below).

As generally is for I=3/2 nuclei with no static spectral splitting and dominantly quadrupolar relaxation, the transverse relaxation behavior for ^{7}Li must be inherently double-exponential (that is, a two-component relaxation decay) if motions with correlation time longer than the inverse of the involved Larmor frequency are present. Moreover, in that case the T_2 of the slowly decaying component should become similar in value to the value of T_1.[44,45] This is clearly not the case for the ^{7}Li relaxation in either of the samples: the relaxation decay observed in spin-echo experiment is not double-exponential but slightly modulated and its estimated decay time (T_2) is shorter by two orders of magnitude than that would be expected on the basis of the T_1 data in **Fig. 2**. These observations jointly indicate that one of the original assumptions – no static spectral splitting in the ^{7}Li spectrum – is invalid. On the other hand, the ^{7}Li spectrum presents no distinct peaks but just a large broadening. To obtain all aspects of the observed behavior, we must assume that there is a broad distribution of small static quadrupole splittings in the ^{7}Li spectra. In such case, the line width is, in a spin echo experiment, dominated by the distribution of static quadrupole couplings.[46]

The systems experience a static quadrupole coupling if they are anisotropic. In polymeric or liquid crystalline systems, the size of the detected splitting depends on the orientation distribution that defines the (local) order parameter and the corresponding main orientation. For ^{7}Li, the presence of a non-zero order parameter depends on the local orientation of the coordinating species – hence, polymer chains within these domains must exhibit some degree of local alignment. If the size of the domains with the same orientation is small, the diffusing species experience a zero average orientation and the static quadrupole splitting vanishes.[47] In our case, the fact that we detect a distribution of static splittings indicates that the diffusion path length during a time comparable to the transverse relaxation time is smaller than the domain size; in other words: the static quadrupole splitting is not averaged to zero by diffusion. In $P(TMC_{20}CL_{80})_{4.6}LiTFSI$, the ^{7}Li diffusion coefficient (see below) and the apparent T_2 value set the lower limit of domain size as $L_D > (6DT_2)^{-1/2} \sim 100$ nm. Previous studies have suggested a hindrance of ion dynamics or complexation in immobilized domains of polyester ionomers and block co-polymers.[48-51]

In line with previous studies,[50,51] we have investigated if the domains inferred from the ^{7}Li spin-echo data also have an influence on translational dynamics. Hence, we recorded, for the anion, the variation of obtained diffusion coefficients D with increasing diffusion time Δ set in the experiments (see **Fig. S2**). We found that at short diffusion times, D decreased with increasing Δ. This feature is a signature of having structural heterogeneities with domains that experience limited connection to each other.[49,51] Although the origin of this feature is yet unclear, it could potentially cause disruption in the ionic transport pathways in the material. The value Δ = 200 ms above which the obtained D reached a stable long-range average value yields an estimate of $L_D \sim$ 400 nm for the domain size. This is consistent with the lower limit of domain size as obtained earlier from the ^{7}Li spin-echo experiments. Note that the ^{7}Li diffusion experiments (see results in self-diffusion coefficients section below) were performed only at Δ = 400 ms, and there we obtained the long-range average value of the diffusion coefficient of the lithium ion.

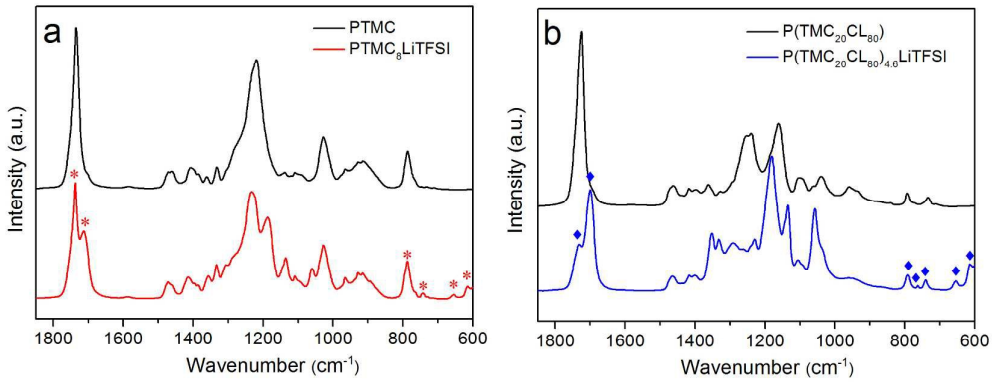

Fig. 4 FTIR spectra of (a) pure PTMC and $PTMC_8LiTFSI$; (b) pure $P(TMC_{20}CL_{80})$ and $P(TMC_{20}CL_{80})_{4.6}LiTFSI$ in the 1850–600 cm^{-1} region. The peaks of interest are particularly marked with symbols: star for PTMC and diamond for $P(TMC_{20}CL_{80})$.

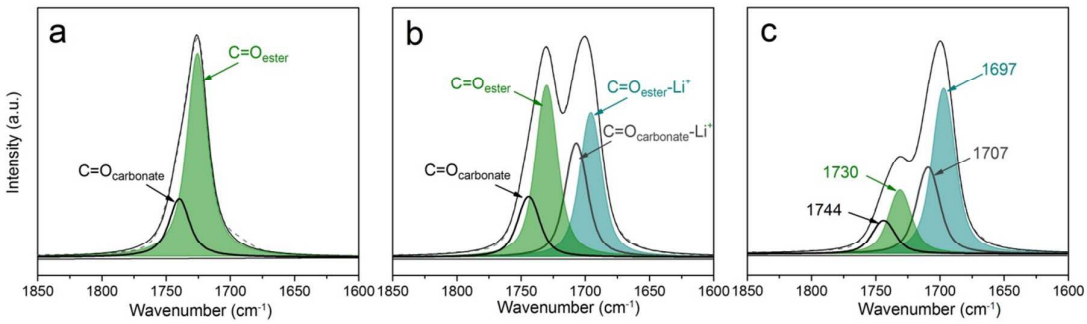

Fig. 5 FTIR spectra of (a) pure $P(TMC_{20}CL_{80})$; (b) $P(TMC_{20}CL_{80})_{6.6}LiTFSI$ and (c) $P(TMC_{20}CL_{80})_{4.6}LiTFSI$ in the 1850–1600 cm^{-1} region. The dashed line represents the sum of the fitted peaks and the fitted spectra are marked in green for $\upsilon_s(C{=}O_{ester})$ and blue for $\upsilon_s(C{=}O_{ester})$–$Li^+$.

FTIR spectroscopy analysis

The IR spectra of $PTMC_8LiTFSI$, $P(TMC_{20}CL_{80})_{6.6}LiTFSI$, and $P(TMC_{20}CL_{80})_{4.6}LiTFSI$ all have the same most notable feature; the intense ν_s(C=O) symmetric carbonyl stretching at 1735 cm^{-1} in pure PTMC and at 1726 cm^{-1} in the pure co-polymer (**Fig. 4**). In the pure co-polymer (**Fig. 5a**), the peak can be deconvoluted into two components due to the ester and carbonate groups, respectively. The area ratio 78:22 is in reasonable agreement with the composition (80:20), which indicates similar absorption coefficients for the two functional groups.

The interactions with the carbonyl oxygen atoms are expected to account for the main contribution to Li^+ coordination and solvation, as previously shown for LiTFSI–ethylene carbonate electrolytes.[16] The carbonyl stretching vibration is very sensitive to Li^+ coordination, shifting to lower wavenumbers, and can furthermore be deconvoluted into ester and carbonate contributions, respectively (**Fig. 5**).[52] The ratio in the SPE, however, no longer corresponds to the 80:20 ratio for the co-polymer, even when both coordinated and un-coordinated carbonyl groups are taken into account. This indicates that the (relative) absorption coefficients may have changed. Furthermore, the peak area ratio between the two different uncoordinated carbonyls notably decreases as more salt is added, from 74:26 for $P(TMC_{20}CL_{80})_{6.6}LiTFSI$ to 66:34 for $P(TMC_{20}CL_{80})_{4.6}LiTFSI$, suggesting that Li^+ preferentially coordinates to ester carbonyl oxygen atoms rather than carbonate carbonyl oxygen atoms. This can either be an effect of inherently stronger complexation or a chelating effect

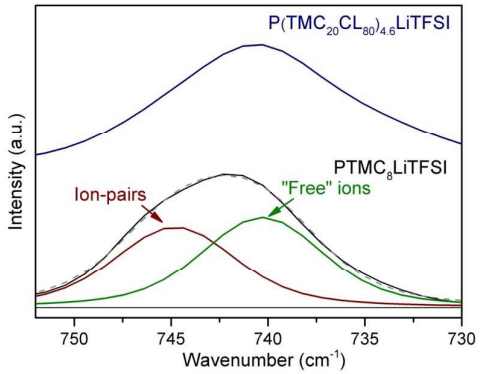

Fig. 6 FTIR spectra of $P(TMC_{20}CL_{80})_{4.6}LiTFSI$ and $PTMC_8LiTFSI$ in the 752–730 cm^{-1} region. The peaks at 740 cm^{-1} and 745 cm^{-1} correspond to the "free" ions and ion-pairs, respectively. The dashed line represents the sum of the fitted peaks.

related to a more regular spacing between ester groups, as opposed to the carbonate groups, in the randomly distributed co-polymer backbone. Both these effects could explain why the addition of a moderate amount of carbonate repeating units leads

to an increase in the ionic conductivity, despite the higher molecular flexibility of PCL as compared to PTMC.[27]

As shown in **Fig. 6**, a group of peaks within 600–800 cm^{-1} are related to the TFSI anions which are sensitive to ion association effects in LiTFSI based SPEs. Those at 600–618 cm^{-1} correspond to the in-plane and out-of-plane asymmetric stretching modes of the SO_2 groups. The peak at 740 cm^{-1} is assigned to an expansion/contraction mode of the "free" TFSI ion,[53] while the Li–TFSI ion-pairs are often found slightly up-shifted: 742–746 cm^{-1}.[53–55] $PTMC_8$LiTFSI shows extensive ion-pairing with a "free" ion peak component at 740 cm^{-1} and a prominent ion-pair component at 745 cm^{-1} and using the peak areas, *ca.* 47% of the TFSI anions are involved ion-pairs. In contrast, the spectrum of $P(TMC_{20}CL_{80})_{4.6}$LiTFSI shows no signs of ion-pairs being present as only the peak centered at 740 cm^{-1} is seen, although with a much larger line width, possibly due to heterogeneities. Again, this could be related to a stronger coordination of Li^+ by the ester carbonyl

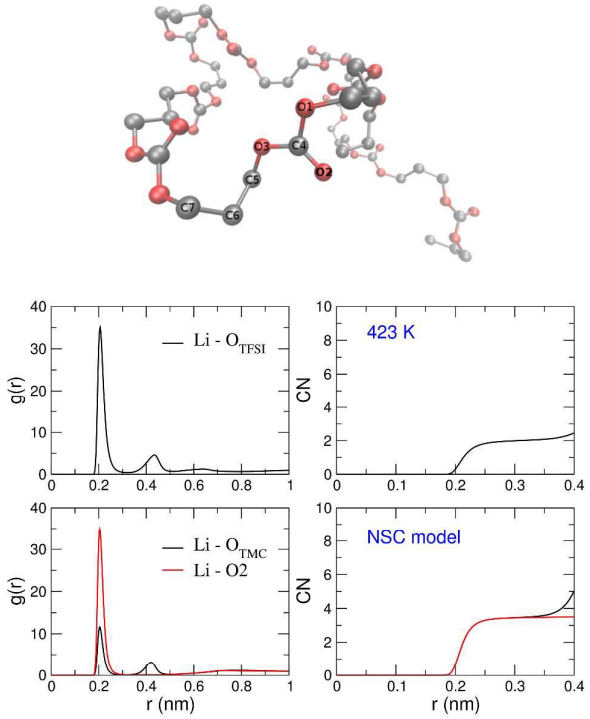

Fig. 7 Top: Nomenclature of PTMC, in which O2 refers to the carbonyl oxygen. Bottom: Radial distribution functions, g(r) and the coordination number (CN) function of Li^+–O_{TFSI} and Li^+–O_{PTMC},as well as Li^+-carbonyl oxygen (O2) in $PTMC_8$LiTFSI simulated from a non-scaled charge (NSC) model at 423 K.

oxygen atoms from the co-polymer chain with concomitant exclusion of the TFSI anions from the first solvation shell.

Structural properties from MD simulations

The coordination environment of ions and ion-polymer interactions was investigated by MD. **Fig. 7** shows the obtained radial distribution functions (RDFs) of the Li–$O_{polymer}$ and Li–O_{TFSI} interactions and the corresponding coordination number (CN) for both electrolyte systems. As shown from RDFs for $PTMC_8$LiTFSI at 423 K, the first and the second coordination shells are positioned at *ca.* 0.21 nm and 0.42 nm, respectively. A dominating Li^+–$O_{polymer}$ coordination can generally be seen, where the Li ions are primarily coordinated to the carbonyl oxygens (O2). In $PTMC_8$LiTFSI, the average total CN of oxygen atoms in the first coordination shell of a Li ion at various temperatures is approximately 5.5 (**Fig. S4**), consisting of 4 carbonyl oxygen atoms and 1–2 oxygen atoms from the TFSI anions. This is generally in agreement with the experimental observations; *i.e.,* Li ions preferably couple to the polymer chains rather than to the TFSI anions. As the temperature increases, the coordination between Li^+ and O_{PTMC} is less influenced as compared to the Li^+–$TFSI^-$ coordination. A stronger ion-pairing can be observed from 303 K to 423 K.

In comparison, **Fig. 8** demonstrates a preferential coordination of Li^+–$O2_{CL}$ with a CN≈3 at 423 K. This is consistent with the discussions on the favorable interaction between the cation and ester carbonyl oxygen atoms from the IR spectroscopy. Also, there is a slight shift of Li^+-O_{CL} and the ratio of CN values for Li^+–$O2_{CL}$ and Li^+–$O2_{TMC}$ is approximately 7. This indicates a stronger coordination to ester carbonyl oxygen atoms than carbonate carbonyl oxygen atoms which further supports the interpretation of the IR data. The coordination of the cation by carbonate groups in TMC and CL units, *i.e.*, Li^+–$O1_{TMC}$ and Li^+–$O1_{CL}$, is minor with no obvious difference between the two.

Transference number and self-diffusion coefficients

The lithium transference number of $PTMC_8$LiTFSI from potentiostatic polarization experiments is obtained as:[29,56]

$$t_+ = \frac{I_{ss}(\Delta V - I_0 R_0)}{I_0(\Delta V - I_{ss} R_{ss})}$$

where ΔV is the potential bias, I_0 and I_{ss} are the initial and steady-state currents, and R_0 and R_{ss} are the initial and steady-state resistances, respectively, measured before and after polarization is applied.

The data in **Fig. 9** provide t_+ ~ 0.80 for $PTMC_8$LiTFSI at 333 K, a value somewhat higher than that of $P(TMC_{20}CL_{80})_{4.6}$LiTFSI presented previously (*i.e.*, 0.66 at 333 K).[27] Similarly high cationic transference numbers were recently found in salt-concentrated poly(ethylene carbonate)–LiTFSI SPEs.[57] The lower t_+ for the co-polymer system fits well with the indications of stronger Li^+ coordination by the ester groups of the co-polymer as compared to the carbonate groups of the TMC repeating units. Stronger complexation naturally leads to impeded cation movements and a lower t_+. However, these transference numbers are still much higher than what is typical for polyether-based SPEs, *e.g.*, 0.1–0.2 for PEO–LiTFSI in the temperature range of 323 K to 363 K using the same method.[27,29] This indicates that polycarbonate host materials provide superior cation transport properties compared to the polyether hosts, where too strong cation coordination results in the anions being

responsible for the overwhelming majority of the charge transport.

In addition, the self-diffusion coefficients of ^{7}Li and ^{19}F at elevated temperatures (323–333 K) were measured by diffusion NMR experiments. Consistent room temperature measurement results were, however, difficult to achieve even with strong magnetic field gradients (up to 15 T/cm). As also addressed in earlier studies comparing transference numbers obtained from NMR and electrochemical methods,[58] contradictory results can be due to contributions from poorly dissociated ion pairs and clusters not avoided in NMR measurements. Therefore, a better comparison may be between MD simulation data and NMR diffusion results. **Fig. 10** shows both the simulated and experimentally determined self-diffusion coefficients. Details on how the self-diffusion coefficients were extracted from MD studies are described in the Supporting Information (**Fig. S3** and **Table S2**). In general larger self-diffusion coefficients, by *ca.* one order of magnitude, were obtained anomalous diffusion coefficient values. Excluding the use of expensive methods via polarizable force-fields, the approximation to the atomic polarizabilities using non-polarizable force-fields may be compensated by a suitable choice of a scaling factor.[60] The limited knowledge about the modeling of polycarbonate-based systems certainly calls for further development of force fields and optimal parameterization. Moreover, MD simulations of SPEs have to be run for considerable time at elevated temperature before leaving the sub-diffusive domain, which is necessary for predicting realistic diffusion coefficient values.[15] Considering the relaxation results discussed above in **Fig. 3**, limited ion transport between domains may lower the observed diffusion coefficient. On the other hand, some useful qualitative information can still be extracted; **Fig. 10** confirms a generally dominant role of the anion diffusion over the cations as seen from both NMR and MD results (in five of the six simulations), which is expected since the anion motions were found

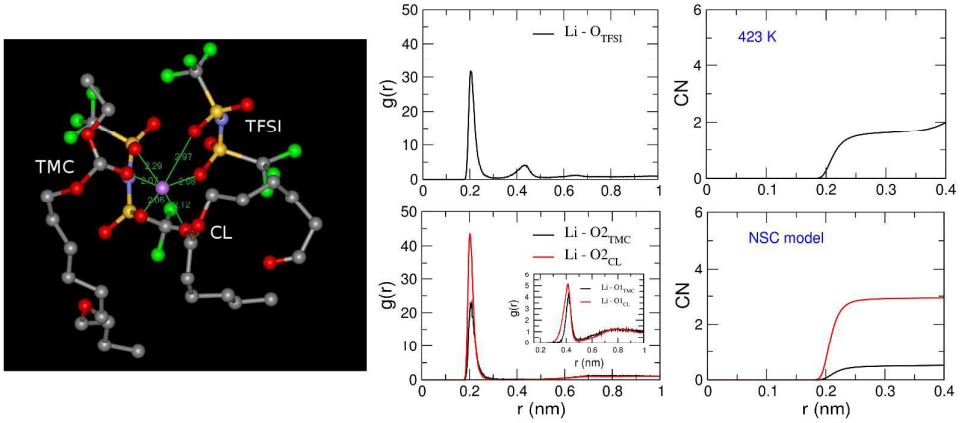

Fig. 8 Left: A snapshot from the equilibrium MD structure showing the local environment interaction between the Li^+ and oxygens from both the anion and the copolymer chain of $P(TMC_{20}CL_{80})_{4.6}LiTFSI$; Right: g(r) and CN function of Li^+–O_{TFSI} , Li^+–$O2_{TMC}$ and Li^+–$O2_{CL}$ in the copolymer system simulated at 423 K. The corresponding g(r) of Li^+–$O1_{TMC}$ and Li^+–$O1_{CL}$ are included in the inset.

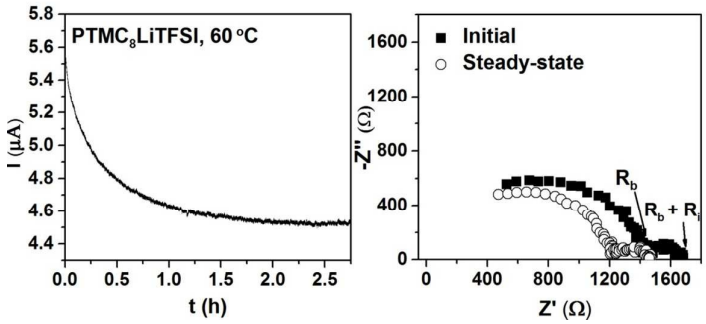

Fig. 9 Left: Potentiostatic polarization of Li/$PTMC_8LiTFSI$/Li under a dc bias of 10 mV; Right: Nyquist plots of the same cell under open circuit and polarized conditions at 333 K.

from the MD simulations. The reasons for this quantitative discrepancy are manifold. It has been addressed that the use of the united-atom model can provide reasonable fits considering the structural relaxation of the polymer in PEO-based SPEs.[59] The small size of the Li-ion and the point-charge model may also contribute to less restricted by the polymer dynamics. Different values of lithium transference number were obtained from PP (0.66) and diffusion NMR (0.32) for $P(TMC_{20}CL_{80})_{4.6}LiTFSI$ at 333–348 K. Similar observations were previously reported for a poly(ethylene carbonate)-based system, $PEC_{0.53}LiFSI$,[24] showing higher cationic

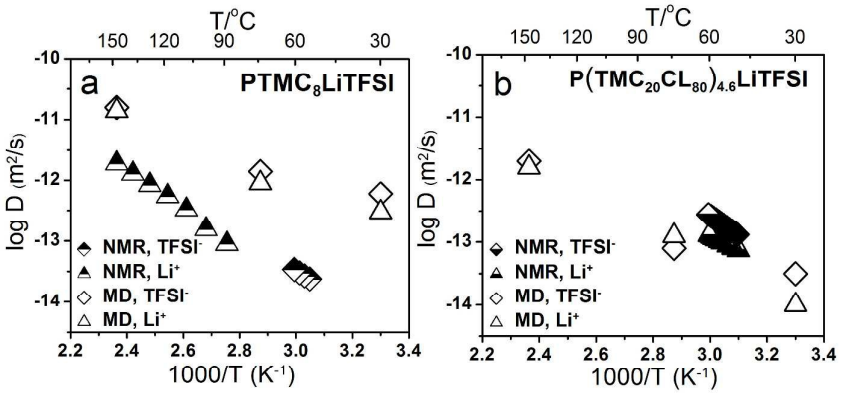

Fig. 10 Self-diffusion coefficients for Li^+, $TFSI^-$ and the polymer from MD simulations (non-filled symbols) and diffusion NMR studies (half-filled symbols) on (a) $PTMC_8LiTFSI$ and (b) $P(TMC/CL)_{4.6}LiTFSI$. The cationic and anionic diffusion coefficients are represented by triangle and diamond symbols, respectively.

transference number by PP than by diffusion NMR (0.54 as compared to 0.24 at 333 K). Considering the limitations of the respective methods for non-ideal electrolytes, ion-association and ion-pair formation play a critical role,[29,58] but the ion transference numbers as detected by NMR cannot exclude this influence. The discrepancy in transference number might be a result of neutral ion aggregates contributing to the overall charge transport.

The polycarbonate–LiTFSI systems being reported so far all displayed higher cationic transference number than for polyether–LiTFSI SPEs.[24,27,61] It has generally been anticipated that ion transport in PEO–LiTFSI systems occurs through Li ions primarily moving with the polymer chain relaxations as they are coordinated to the ether oxygen atoms.[15,62] For PTMC and P(TMC/CL)–LiTFSI, lower donor numbers (DNs) than polyethers are expected. High DNs and optimal spacing between ether oxygen atoms could lead to stable cation–polymer coordination structures.[63] Both esters and carbonates have higher dipole moments than ethers, and generally lower donor numbers than ethers.[64-67] This could translate to an enhancement in dissociation ability, particularly in the co-polymer host, and also less favorable Li–polymer coordination than for ethers. The overall outcome of high cation transference numbers might be due to promoted dissociation by low DNs and high dipole moments,[63,64] assisted by ion-pairs and aggregates playing a transient role in the Li^+ conduction mechanism.

The fitted apparent activation energies for ^{19}F and ^{7}Li from diffusion NMR studies are summarized in the Supporting Information (**Table S3**). It should be mentioned that apparent E_a of translational motion is found to be much higher than those for re-orientational motion (derived from the longitudinal relaxation data). Particularly, the E_a for the re-orientational motion of the ^{7}Li cation is five times lower than the E_a corresponding to the translation motion; *ca.* 13.5 kJ/mol and 65 kJ/mol, respectively, an effect larger than in previous studies.[36] The range of the correlation times from the dominating structure of the co-polymer was also simulated, and estimated to be in the ns range (see **Fig. S5** and **S6**). The re-orientation dynamics of the ionic species were found to be faster than those of the structural relaxation or the translational motion, consistent with the NMR results. Moreover, the E_a of the reorientation motion for ^{7}Li and ^{1}H appear very close to each other. This is strongly correlated with previous studies on SPEs where the following theory is commonly accepted: the local segmental motion of the polymers (often correlating to the α relaxation) can contribute significantly to the lithium ion transport, depicted by lithium ions hopping within cages formed by the polymer chains.[10] In polycarbonate based SPEs, the Li^+ ions coordinated by the carbonyl oxygen atoms might move in a similar tumbling manner as the polymer chain for a short distance, whereas long-range diffusive motion is limited and more energetically demanding. Incorporation of CL chains sufficiently reduces the cation E_a as compared to the PTMC system, while the anion E_a is only weakly affected. This result is consistent with our prediction from the T_1 relaxation data; less restrictions to the ionic motions in the co-polymer matrix. Hence, it may be concluded that the coupling of cation dynamics to the segmental motions of the polymer chains permits the flexible CL units to promote cation diffusion.

Conclusions

This work presents an investigation on the ion transport behavior in SPEs based on non-polyether host material – polycarbonates and polyesters – through both experimental and modeling approaches. FTIR and NMR relaxation studies on PTMC- and $P(TMC_{20}CL_{80})$-based SPEs showed a coupling between the Li ion motions with the segmental movements of the polymer chains. Examination of FTIR spectra of the $P(TMC_{20}CL_{80})$–LiTFSI system as a function of salt concentration indicated a stronger Li^+ coordination to CL monomers than to TMC monomers. The anion motions were found to be only weakly affected when varying the polymer host materials. This could be attributed to the dominant anion diffusion, poorly connected to the polymer motions, as detected by diffusion NMR experiments. Compared to conventional polyether based SPEs, higher lithium transference numbers were obtained for the PTMC-based SPEs. This might be a result of favorable dissociation and less stable Li-polymer coordination structures. In addition, MD simulations demonstrated the Li ion coordination to be primarily to the carbonyl ester oxygen atoms, in agreement with the experimental observations. Altogether, these results generally suggest a Li ion transport mechanism involving cation movement

coupled to the segmental motions of the polymer chains. However, the observations of preferential coordination to ester moieties clearly indicate both the complexity and potential of introducing ester groups to polycarbonate systems. Stronger Li^+-ester oxygen coordination could reduce the "free" ion fractions and thus lower the transference number. The balance between strongly and more weakly complexing constituents coupled with their respective molecular flexibility provides a key towards tailoring new polymer host materials for improved ion transport dynamics. This could be achieved by for example chemical modifications which plasticize the TMC repeating unit and/or weakens the ion complexation strength of the CL monomer. For both polymers, we established that there exists locally oriented domains that are a few hundred nanometers large and between which the ionic transport is to some extent limited. There should thus be ample room for further improvement of ion transport properties in SPEs by proper utilization of the full potential of alternative polymer host systems beyond the polyether paradigm.

Acknowledgements

This project has been funded by STandUP for Energy, the Swedish Research Council (VR) (grant no. 2012-3837 and 2012-3244), the Carl Tryggers Foundation, and the Swedish Foundation for Strategic Research (SSF). The authors wish to thank Prof. Michel Armand at CIC Energigune for fruitful discussions.

References

1 M. Tarascon, J.-M., Armand, *Nature*, 2001, **414**, 359–367.
2 D. T. Hallinan and N. P. Balsara, *Annu. Rev. Mater. Res.*, 2013, **43**, 503–525.
3 K. Xu, *Chem. Rev.*, 2014, **114**, 11503–11618.
4 K. Xu, *Chem. Rev.*, 2004, **104**, 4303–4417.
5 S. E. Sloop, J. B. Kerr and K. Kinoshita, *J. Power Sources*, 2003, **119-121**, 330–337.
6 E. Quartarone and P. Mustarelli, *Chem. Soc. Rev.*, 2011, **40**, 2525–2540.
7 R. C. Agrawal and G. P. Pandey, *J. Phys. D. Appl. Phys.*, 2008, **41**, 223001 (1–18).
8 M. B. Armand, *Annu. Rev. Mater. Res.*, 1986, **16**, 245–261.
9 J. W. Fergus, *J. Power Sources*, 2010, **195**, 4554–4569.
10 M. A. Ratner, P. Johansson and D. F. Shriver, *MRS Bull.*, 2000, 31–37.
11 W. Gorecki, M. Jeannin, E. Belorizky, C. Roux and M. Armand, *J. Phys. Condens. Matter*, 1995, **7**, 6823–6832.
12 O. Borodin and G. D. Smith, *J. Phys. Chem. B*, 2006, **110**, 4971–4977.
13 P. Johansson, J. Tegenfeldt and J. Lindgren, *Polymer*, 1999, **40**, 4399–4406.
14 G. Mao, M. L. Saboungi, D. L. Price, M. B. Armand and W. S. Howells, *Phys. Rev. Lett.*, 2000, **84**, 5536–5539.
15 O. Borodin and G. D. Smith, *Macromolecules*, 2006, **39**, 1620–1629.
16 O. Borodin, G. D. Smith and P. Fan, *J. Phys. Chem. B*, 2006, **110**, 22773–22779.
17 D. Golodnitsky and E. Peled, *Electrochim. Acta*, 2000, **45**, 1431–1436.
18 D. Brandell, A. Liivat, A. Aabloo and J. O. Thomas, *J. Mater. Chem.*, 2005, **15**, 4338–4345.
19 Y. Wang and A. P. Sokolov, *Curr. Opin. Chem. Eng.*, 2015, **7**, 113–119.
20 P. V. Wright, Y. Zheng, D. Bhatt, T. Richardson and G. Ungar, *Polym. Int.*, 1998, **47**, 34–42.
21 R. Idris, M. D. Glasse, R. J. Latham, R. G. Linford and W. S. Schlindwein, *J. Power Sources*, 2001, **94**, 206–211.
22 M. Forsyth, J. Sun, D. R. MacFarlane and A. J. Hill, *J. Polym. Sci. Part B Polym. Phys.*, 2000, **38**, 341–350.
23 C. A. Angell, C. Liu and E. Sanchez, *Nature*, 1993, **362**, 137–139.
24 Y. Tominaga and K. Yamazaki, *Chem. Commun.*, 2014, **50**, 4448–4450.
25 B. Sun, J. Mindemark, K. Edström and D. Brandell, *Solid State Ionics*, 2014, **262**, 738–742.
26 B. Sun, J. Mindemark, K. Edström and D. Brandell, *Electrochem. Commun.*, 2015, **52**, 71–74.
27 J. Mindemark, B. Sun, E. Törmä and D. Brandell, *J. Power Sources*, 2015, **298**, 166–170.
28 J. Mindemark, E. Törmä, B. Sun and D. Brandell, *Polymer*, 2015, 63, 91–98.
29 M. M. Hiller, M. Joost, H. J. Gores, S. Passerini and H.-D. Wiemhöfer, *Electrochim. Acta*, 2013, **114**, 21–29.
30 J. Evans, C. A. Vincent and P. G. Bruce, *Polymer*, 1987, **28**, 2324–2328.
31 S. J. Gibbs and C. S. Johnson, *J. Magn. Reson.*, 1991, **93**, 395–402.
32 J. T.-R. W. L. Jorgensen, D. S. Maxwell, *J. Am. Chem. Soc.*, 1996, **118**, 11225–11236.
33 T. I. Morrow and E. J. Maginn, *J. Phys. Chem. B*, 2002, **106**, 12807–12813.
34 S. Pronk, S. Páll, R. Schulz, P. Larsson, P. Bjelkmar, R. Apostolov, M. R. Shirts, J. C. Smith, P. M. Kasson, D. van der Spoel, B. Hess and E. Lindahl, *Bioinformatics*, 2013, **29**, 845–854.
35 L. Martínez, R. Andrade, E. G. Birgin and J. M. Martínez, *J. Comput. Chem.*, 2009, **30**, 2157–2164.
36 M. Kunze, A. Schulz, H.-D. Wiemhöfer, H. Eckert and M. Schönhoff, *Z. Phys. Chem.*, 2010, **224**, 1771–1793.
37 C. Neagu, J. E. Puskas, M. A Singh and A. Natansohn, *Macromolecules*, 2000, **33**, 5976–5981.
38 S. W. Chen and P. J. Rossky, *J. Phys. Chem.*, 1993, **97**, 10803–10812.
39 K. Hayamizu, Y. Aihara and W. S. Price, *J. Chem. Phys.*, 2000, **113**, 4785–4793.
40 N. Bloembergen, E. M. Purcell and R. V Pound, *Phys. Rev.*, 1948, **73**, 679.
41 C. Roux, W. Gorecki, J.-Y. Sanchez, M. Jeannin and E. Belorizky, *J. Phys. Condens. Matter*, 1999, **8**, 7005–7017.
42 A. Kuhn, S. Narayanan, L. Spencer, G. Goward, V. Thangadurai and M. Wilkening, *Phys. Rev. B*, 2011, **83**, 094302 (1–11).

43 G. M. Mao, R. F. Perea, W. S. Howells, D. L. Price and M. L. Saboungi, *Nature*, 2000, **405**, 163–165.

44 P. H. Kenéz, G. Carlström, I. Furó and B. Halle, *J. Phys. Chem.*, 1992, **96**, 9524–9531.

45 P. S. Hubbard, *J. Chem. Phys.*, 1970, **53**, 985–987.

46 I. Furó, B. Halle and L. Einarsson, *Chem. Phys. Lett.*, 1991, **182**, 547–550.

47 D. Bernin, V. Koch, M. Nydén and D. Topgaard, *PLoS One*, 2014, **9**, e98752 (1–11).

48 P. M. Carrasco, A. Ruiz De Luzuriaga, M. Constantinou, P. Georgopanos, S. Rangou, A. Avgeropoulos, N. E. Zafeiropoulos, H. J. Grande, G. Cabañero, D. Mecerreyes and I. Garcia, *Macromolecules*, 2011, **44**, 4936–4941.

49 V. M. Litvinov, A. W. M. Braam and A. F. M. J. van der Ploeg, *Macromolecules*, 2001, **34**, 489–502.

50 K. Hayamizu, E. Akiba and W. S. Price, *Macromolecules*, 2003, **36**, 8596–8598.

51 K. Hayamizu, K. Sugimoto, E. Akiba, Y. and W. S. Price, *J. Phys. Chem. B*, 2002, **106**, 547–554.

52 K. Hongyou, T. Hattori, Y. Nagai, T. Tanaka, H. Nii and K. Shoda, *J. Power Sources*, 2013, **243**, 72–77.

53 I. Rey, P. Johansson, J. Lindgren, J. C. Lassègues, J. Grondin and L. Servant, *J. Phys. Chem. A*, 1998, **102**, 3249–3258.

54 P. Johansson, J. Tegenfeldt and J. Lindgren, *J. Phys. Chem. A*, 2000, **104**, 954–961.

55 L. Edman, *J. Phys. Chem. B*, 2000, **104**, 7254–7258.

56 N. A. Stolwijk, J. Kösters, M. Wiencierz and M. Schönhoff, *Electrochim. Acta*, 2013, **102**, 451–458.

57 K. Kimura, H. Matsumoto, J. Hassoun, S. Panero, B. Scrosati and Y. Tominaga, *Electrochim. Acta*, 2015, **175**, 134–140.

58 S. Zugmann, M. Fleischmann, M. Amereller, R. M. Gschwind, H. D. Wiemhöfer and H. J. Gores, *Electrochim. Acta*, 2011, **56**, 3926–3933.

59 L. J. A. Siqueira and M. C. C. Ribeiro, *J. Chem. Phys.*, 2006, **125**, 214903 (1–8).

60 L. T. Costa, B. Sun, F. Jeschull and D. Brandell, *J. Chem. Phys.*, 2015, **143**, 024904 (1–9).

61 Y. Tominaga, K. Yamazaki and V. Nanthana, *J. Electrochem. Soc.*, 2015, **162**, A3133–A3136.

62 C. Do, P. Lunkenheimer, D. Diddens, M. Götz, M. Weiß, A. Loidl, X.-G. Sun, J. Allgaier and M. Ohl, *Phys. Rev. Lett.*, 2013, **111**, 018301 (1–5).

63 C. S. Kim and S. M. Oh, *Electrochim. Acta*, 2000, **45**, 2101–2109.

64 V. Gutmann, in *Coordination Chemistry in Non-Aqueous Solutions*, Springer-Verlag, 1968, p. 19.

65 B. A. Arbuzov, I. V Anonimova, L. L. Tuzovs, V. A. Naumov, E. G. Yarkova, N. R. Safiullina, A. P. Timosheva, A. N. Vereshchagin, *Bull. Acad. Sci. USSR, Div. Chem. Sci.*, 1985, **33**, 2476–2481.

66 R. C. Weast, Ed., *CRC Handbook of Chemistry and Physics*, 85th Edition, 1964.

67 T. Ohhashi, M. Takahama, T. Eto, D. Mori, S. Yokoi, US 8354365 B2, Jan.15, 2013.